RECENT RESULTS ON THE PROBLEM OF WAVE-CURRENT INTERACTION INCLUDING WATER DEPTH, SURFACE TENSION/AMPLITUDE AND VORTICITY EFFECTS

Philippe Maïssa[1], Germain Rousseaux[2] and Yury Stepanyants[3]

Abstract

A brief review on wave–current interaction is presented. The simplest model of vortical shear flow – the current with a linearly varying velocity with depth is considered and results obtained are compared with the uniform current case. Different scenarios of wave blocking depending on the Froude number and other governing parameters (water depth, surface tension, vorticity) are discussed in details. The weakly nonlinear effects are also taken into consideration, while the majority of presented results were obtained in the linear approximation.

Key words: Wave-Current Interaction. Blocking Phenomenon. Water Depth. Surface Tension. Shear Flow. Vorticity.

1. Introduction

Coastal processes often feature the combined effects of waves, currents and sediment transport interacting together. For example, sand ripples are formed due to synergetic effect of waves and currents. In this communication we focus on the interaction between water waves and steady currents inhomogeneous in space. Surface waves in a coastal zone can strongly interact with currents of any nature, such as tidal, wind-generated, produced by oceanic circulations, generated by swells or by river inflows, etc. Currents may produce dramatic effects such as rip generation due to wave-bathymetry interaction or rogue waves generation due to wave-current interaction. The derivation of basic equations describing wave-current interaction has quite old history; we can't refer here to all publications in this field and indicate only few, the most relevant to the topic (Peregrine, 1976; Jonsson, 1990; Thomas & Klopman, 1997).

When the flow current varies slowly in space, the main kinematic effects of wave propagation can be deduced from the dispersion relation between the wave frequency and wave number. In the presence of gradually varying current such dispersion relation contains variable parameters. This allows us grasping the essential physical features of wave-current interaction, in particular, the blocking of waves, amplitude variations or the wavenumber shift. Here, we neglect strong non-linear effects and back-reaction of waves on currents. The present paper represents a survey of results on wave-current interaction and aims to deliver the recent achievements in this field to the broad community of coastal zone oceanographers. Details of results derivation can be found in the related bibliography. We will focus mainly on the interaction between surface water waves and counter-propagating currents; in such arrangement there is a rich variety of non-trivial physical effects. The analysis of the dispersion relation leads to the space of parameters where the blocking velocity of the current is expressed as a function of a period of incoming wave (Nardin et al., 2009; Rousseaux et al., 2010; Rousseaux, 2011). Several plots illustrating outcomes of such analysis are presented below. The effects of vorticity, water depth and surface tension, as well as finite amplitude of waves were taken into consideration (Maïssa et al., 2013).

[1]CNRS UMR 7351, Laboratoire Dieudonné, University of Nice, Parc Valrose, Nice 06300, France.
philippe.maissa@unice.fr
[2]CNRS UPR 3346, Institut Pprime, 11 Bd Marie et Pierre Curie, Futuroscope 86962, France.
germain.rousseaux@univ-poitiers.fr
[3] University of Southern Queensland, Department of Mathematics and Computing, Toowoomba, Australia.
yuas50@gmail.com

2. The physics of wave-current interaction

The first and simplest effect of a current on water waves is a shift in the wavenumber. When a wave co-propagates with a current, its *wavelength* increases. This effect is dubbed the redshifting by analogy with optics when the *period* of electromagnetic wave increases due to certain effects (Doppler effect, or red-shift effect in cosmology). Analogously, when a wave counter-propagates with a current, it experiences the blueshifting due to its *wavelength* decreases. In addition to that, counter-current propagating waves induce a mode conversion already in the linear approximation: an incident wave interacting with the current produces co- and counter propagating waves with different wavenumbers but with the same frequency in the immovable coordinate frame. The third effect of wave-current interaction is wave blocking when the incident wave can be stopped by a sufficiently strong current. This may happen when the group velocity of a wave defined by the slope of the dispersion relation vanishes and the wave cannot penetrate over the blocking point. The fourth effect is such that the energy of incoming wave is not conserved; it converts into other modes. However, it can be shown that the wave-action flux is conserved: that is the product of wave energy by the group velocity divided by the *relative frequency* remains constant. The latter quantity is of the utmost importance characterizing the physical processes involved in the wave-current interaction. Indeed, the relative frequency is the frequency in the coordinate frame co-moving with the fluid (for the sake of simplicity we presume here that fluid velocity is uniform in depth). One can show that the total energy of a sinusoidal wave averaged over a period is proportional to the relative frequency. Hence, waves with positive/negative relative frequency are by definition waves with positive/negative energy (we use the acronyms PEWs for positive energy waves and NEWs for negative energy waves, see, e.g., Nezlin, 1976; Ostrovsky et al., 1986; Stepanyants & Fabrikant, 1989; Fabrikant & Stepanyants, 1997).

Here, we will study the conversion of PEWs into others PEWs and NEWs in the presence of dispersive effects caused by water depth and surface tension, as well as amplitude and vorticity effects. As the wave energy in the linear approximation is proportional to the square of the wave amplitude, it is obvious that it diverges when the wave reaches the wave blocking point where the group velocity vanishes. Indeed, due to conservation of the wave-action flux, the product of wave energy and group velocity is constant. Hence, the appearance of freak waves on counter-propagating current in the coastal regions, for example, is easily understood.

Waves on uniform flows were studied since the 19th century. The first non-trivial dispersion relation with the vorticity effect was derived by Thompson (1949) and Biesel (1950) for the shear flow linearly varying with depth: $U(z) = U_0 + \Omega z$. The vorticity in such shear flow is constant and equals to Ω. The dispersion relation for waves in a water layer of depth h reads:

$$\omega = U_0 k - \frac{\Omega}{2}\tanh kh \pm \sqrt{\left(\frac{\Omega}{2}\tanh kh\right)^2 + \left(gk + \frac{\gamma}{\rho}k^3\right)\tanh kh}, \tag{1}$$

where g is the acceleration due to gravity, γ is the surface tension and ρ is the water density (we presume that the physical frequency is non-negative quantity, whereas the wavenumber may be of either sign, positive or negative).

During the World War II, G.I. Taylor studied waves on currents with velocity profiles either constant with depth or linearly varying with depth (both in a finite vertical extension) and derived implicit dispersion relations for such flows (Taylor, 1955) (his work was published after the works of Thompson and Biesel). The idea was to use pneumatic wave-breakers during the D-Day to help in the Normandy ship "landings" operations. Skop (1987) computed an approximate dispersion relation for a jet-like flow. Other shear flows with rather exotic profiles (e.g., exponentially or sinusoidally varying with depth) were also studied in the past (Peregrine, 1976; Jonsson, 1990; Thomas & Klopman, 1997). Recently Karageorgis derived the implicit dispersion relation for the velocity profile of any non-constant vorticity but with the constraint that the relationship between the vorticity and stream function is known (Karageorgis, 2012). Figure 1 resumes different velocity profiles for which the analytical dispersion relations were derived historically.
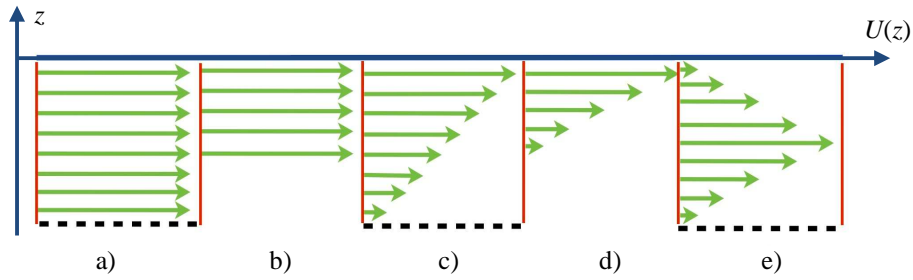
Figure 1. Examples of velocity profiles for which the dispersion relations were derived in analytic form: a) – depth-independent velocity with zero vorticity, b) – piece-constant velocity profile (Taylor-1) with a vortex sheet at the interface between layers, c) – linear velocity profile with constant vorticity (Thompson, Biesel), d) – piece-linear velocity profile (Taylor-2) with the piece-constant vorticity, e) piece-linear velocity profile of a jet-type (Skop) with the piece-constant vorticity of opposite sign.

Here, we will carry out the analysis based on the dispersion relation derived by Thompson and Biesel for linear velocity profile in order to demonstrate with the help of this simplest model the effect of vorticity and compare the results obtained against those derived for constant velocity profile without vorticity.

3. Outcomes from the dimensional analysis

As it is well known, the dimensional analysis is a powerful tool to grasp the simple physics behind any phenomenon. Let us consider water waves of a period T in the gravity field with the acceleration constant g. Water has the density ρ and surface tension γ. The current flowing opposite to propagating waves is supposed to be either uniform with depth with the constant velocity U_0 or linearly varying with depth with the constant vorticity Ω. The water depth h is assumed to be constant. With the help of the dimensional analysis, the typical blocking velocities can be readily derived using either the Vaschy–Buckingham theorem (Barenblatt, 1996) or balance of terms in the dispersion relation (Rousseaux, 2011). These procedures lead to several velocity scales for the blocking velocity U^* (which is assumed to be negative in the considering coordinate frame). In a shallow water the blocking velocity can be expressed as a function of the water depth $U_h = -(g\,h)^{1/2}$, whereas in a deep water it depends only on the wave period $U_g = -g\,T/8\pi$. Here, both the surface tension and flow vorticity were neglected.

If we consider waves of relatively short period on deep water, then the capillary effects with the parameter γ should be taken into account too. Balancing the gravity and surface tension terms in the dispersion relation, one recovers the well-known critical velocity $U_\gamma = -(\gamma g/\rho)^{1/4}$ which corresponds to the minimum of the phase velocity of gravity-capillary waves. Dimensional analysis allows also to anticipate the role of a period scaling with $(h/g)^{1/2}$ when interpreting the results in shallow-water with depth h.
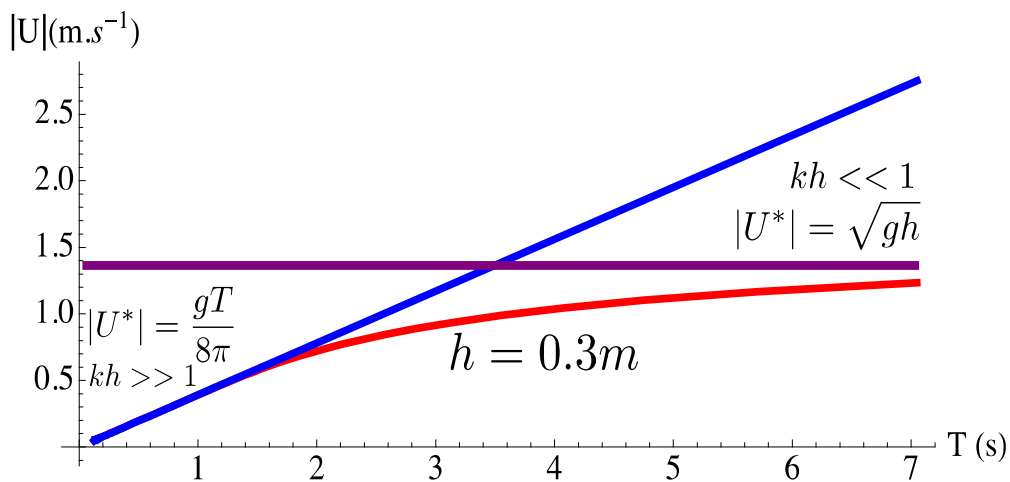

Figure 2. The dependence of blocking velocity for the flow of depth-independent profile when the effects of surface tension and vorticity are neglected.

It is interesting to track the behavior of water waves when meeting an adverse current with a constant velocity profile. This allows one to shed light onto the blocking effect in terms of successive modification of the dispersion relation. Let us take first a deep-water wave to illustrate the process. As we have seen, the wave packet can be stopped if it meets a counter-current $U(x)$ varying in space and achieving the blocking velocity U_g proportional to the period. In a shallow-water the wave packet can be stopped when the counter-current velocity $U(x)$ achieves the critical velocity U_h depending on the water depth only. The period of transition is obtained by equating U_g and U_h that is $T = 8\pi(h/g)^{1/2}$. In the diagram of Figure 2 the deep-water regime occurs at small periods (above straight blue line) whereas the shallow-water regime occurs at large periods (below horizontal purple line). In the case of waves in a fluid of finite depths, the boundary between the deep-water and shallow water regimes is given by red line. In the shallow-water case, it is convenient to determine the wave blocking condition in terms of a critical Froude number $F_r = |U|/|U_h|$.

When propagating against a counter current, the wavelength keeps decreasing until it reaches typical lengths in a cascade such as the water depth or for even smaller scales like the capillary length where new dispersive effects will affect the blocking phenomenology as well as the mode conversion. Here, one must distinguish between the deep-water or the shallow-water asymptotic limits. Indeed, in the shallow water limit, the capillary effect is usually a small correction with respect to the water depth effect in application to coastal zone dynamics. Expanding the dispersion relation into the Taylor series, one can show that in shallow-water the blocking velocity reads (Maïssa et al., 2013):

$$ U^* \approx -\sqrt{gh}\left[1 - \frac{1}{T^{2/3}}\left(\frac{3\sqrt{2}\pi}{2}\sqrt{\frac{h}{g}}\right)^{2/3}\right] \tag{2} $$

One recovers $U_h = -(gh)^{1/2}$ in the long-period limit ($T \to \infty$) corresponding to the extreme shallow regime (see the deviation of red line from the purple asymptote in Figure 2). For even shorter wavelengths, that is for stronger flow current intensity, the wavelength reaches eventually a viscous scale where dissipation strongly affects the waves and eventually suppress them completely. So far we considered only the linear effects. If the flow is sufficiently strong, due to conservation of the wave action the amplitude of wave increases and may modify the dispersion relation or induce wave breaking in extreme regimes. In the deep water, the phenomenology is more complex since the effect of dispersion complicates the mode conversion as will be shown below. It can be noted, however, that in the deep-water regime the effect of surface tension, to a certain extent, is similar to the nonlinear effect caused by large-amplitude perturbation; the corresponding dispersion relation has been proposed, e.g., in the papers (Kirby & Dalrymple, 1986; Chawla & Kirby, 2002). For surface waves on a depth-independent current, the equations read:

$$ (\omega - U_0 k)^2 \approx g|k|\left(1 + \frac{\gamma}{\rho g}k^2\right); \qquad (\omega - U_0 k)^2 \approx g|k|\left(1 + a^2 k^2\right), \tag{3} $$

where ak is the wave steepness, and a is the wave amplitude.

4. The mode conversion

Analysis of the dispersion relation can be easily done in a graphical representation. In deep-water and without surface tension, one knows since a long time that four wavenumbers are solutions of the dispersion relation for a constant frequency provided the velocity is given (Peregrine, 1976). Figure 3 illustrates the dependence of wave frequency against wavenumber for a fixed flow velocity. As one can see, dashed horizontal line intercepts four times the dispersion relation (black points in Fig. 3): three times with the positive green branch and one time with the negative blue branch of the dispersion relation (1). The condition for wave blocking corresponds to the null tangent of the dispersion relation (here, a single maximum: the purple point in Fig. 3).

Now it is easy to understand the mode conversion process in the vicinity of the blocking point. Strictly speaking, all the four solutions always exist on the nonzero counter current whose velocity $U < U^*$. An incident wave propagating against the current transforms into a blue-shifted wave staying on the same positive branch of the dispersion line (see the black point on the top right in the first quadrant of Figure 3).

The process is said to be *adiabatic* and the slowly varying parameter is the current gradually varying in space.

Figure 4 resumes schematically the mode conversion processes underlining the sign of wave energy (here the sign corresponds to the fluxes of energy and direction of group velocity but not to the phase velocity). For example, the incident wave of positive energy (PEW) converses into the reflected blue-shifted PEW whose energy is going backward whereas its crests propagate in the same direction as the incident wave. Other mode conversions are also possible, such as the non-adiabatic one between the positive and negative branch of the dispersion relation leading to generation of reflected NEW (very left black point in the second quadrant of Figure 3). Such mode conversion are well known in electronics for example (Kovalev, 1984).
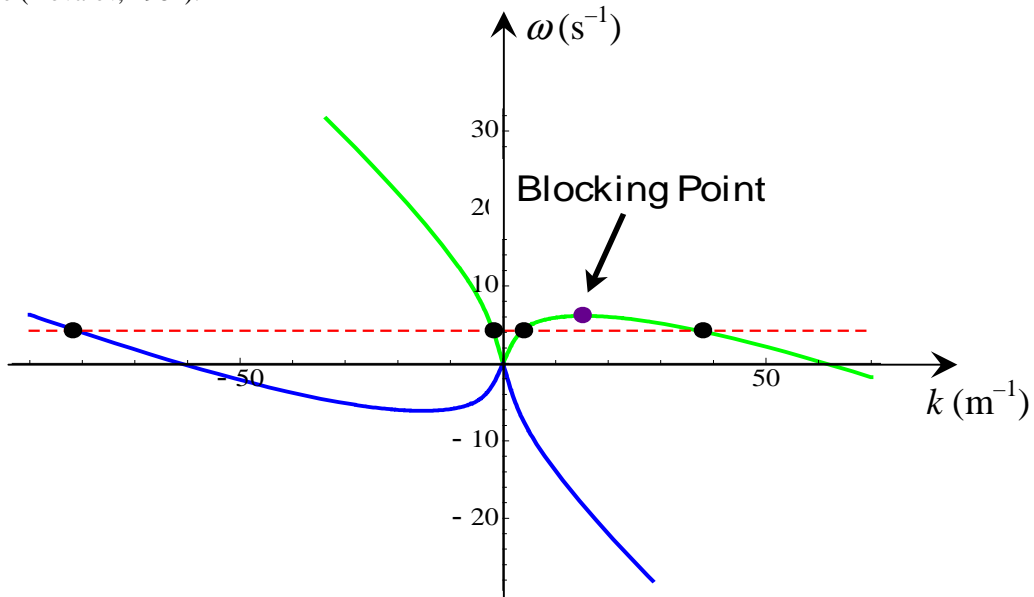

Figure 3. The dispersion relation for water waves in uniformly moving fluid in the pure gravity case on deep-water. For the sake of clearness both positive and negative branches of the dispersion relation are shown, but only part of the branches with $\omega \geq 0$ make sense from the physical point of view.
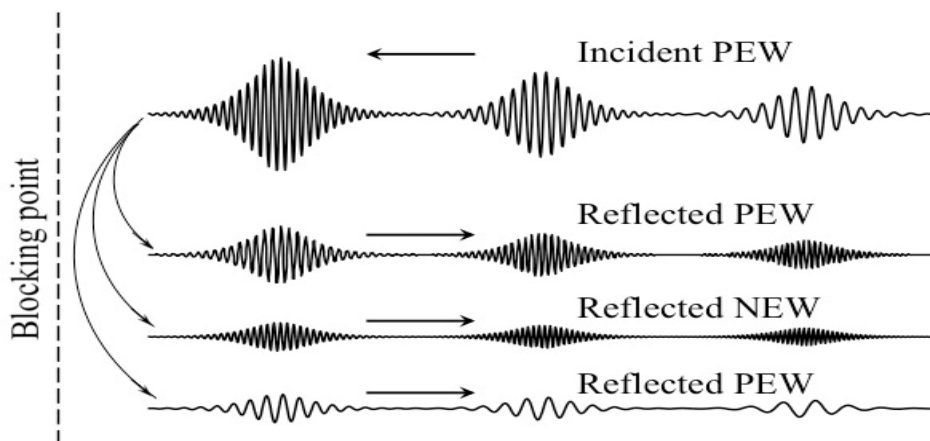

Figure 4. Mode conversion in the pure gravity case at the blocking point for the PEW and NEW.

The inclusion of a surface tension complicates the overall picture. Indeed, in the deep water and without vorticity, no less than six solutions are possible with three blocking points. Figure 5 shows how the dispersion branches evolve when the flow current increases. The blue-shifted waves, which are already present in the pure gravity case, would have drift back reaching a vanishing wavelength in the null velocity

region. To avoid this degeneracy, the capillary length plays the role of a regularizing mechanism allowing new mode conversions and a new blocking point 2 for the blue-shifted waves (see Figure 5), which are transformed into capillary waves and which are no more blocked at the former blocking point 1. Interestingly, the NEW waves are also stopped at a new blocking point 3.

Similarly to the pure gravity case, one can picture the mode conversion processes at the new blocking point 2 or 3 (see Figure 6). For example, the incident gravity-capillary waves PEW in Figure 6 correspond to the reflected gravity PEWs in Figure 4 albeit with a different velocity. The cascading process and the double reflection from incident gravity waves toward capillary waves through blue-shifted waves was observed experimentally long time ago by Badulin et al. (1983). One anticipates the same phenomenology for waves with a finite amplitude in deep-water provided the only correction of non-linearity is restrained to the dispersion relation since one has shown that the capillary length would be replaced by the wave amplitude. Conversions into NEW are also possible but were not displayed in the Figure 6.
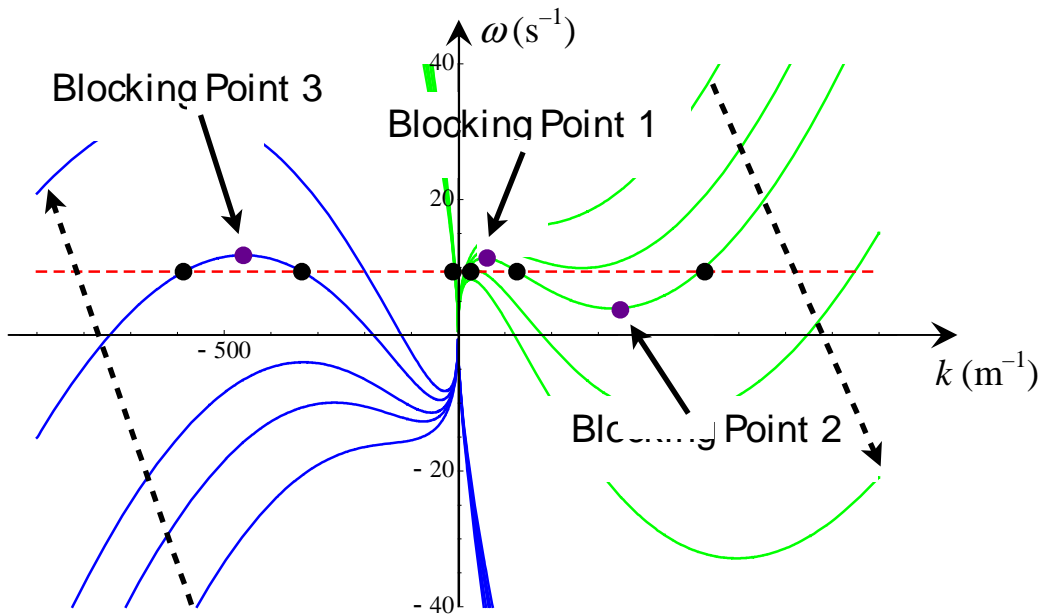

Figure 5. The dispersion relation for the gravity-capillary waves in the deep water. Different lines correspond to different current velocity of uniform profile. The absolute value of the current velocity increases as indicated by the dashed lines.
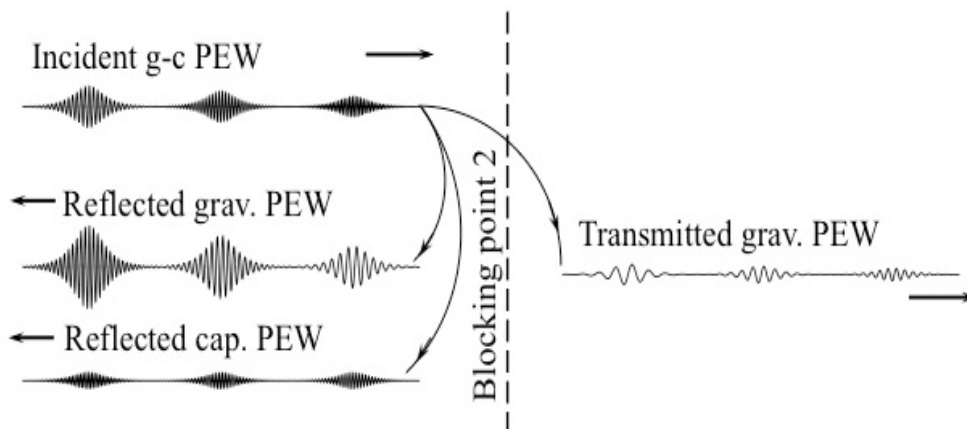

Figure 6. Mode conversion in the case of gravity-capillary waves at the blocking point 2 for the PEWs only.

5. The parameter spaces with the vorticity effect.

The detailed analysis of the dispersion relation allows us to construct the parameter spaces for the blocking phenomenon in terms of the dependence of the Froude number as a function of the wave period, water depth and vorticity (Maïssa et al., 2013). The velocity scalings deduced from the dimensional analysis can be treated as the asymptotic behaviors of blocking lines shown in Figure 7 (red line 1 pertains to the case with zero vorticity) and Figure 8. The effect of vorticity modifies strongly the asymptotes and the global behavior for long-period waves (see blue line 2 in Figure 7 versus red line 1).
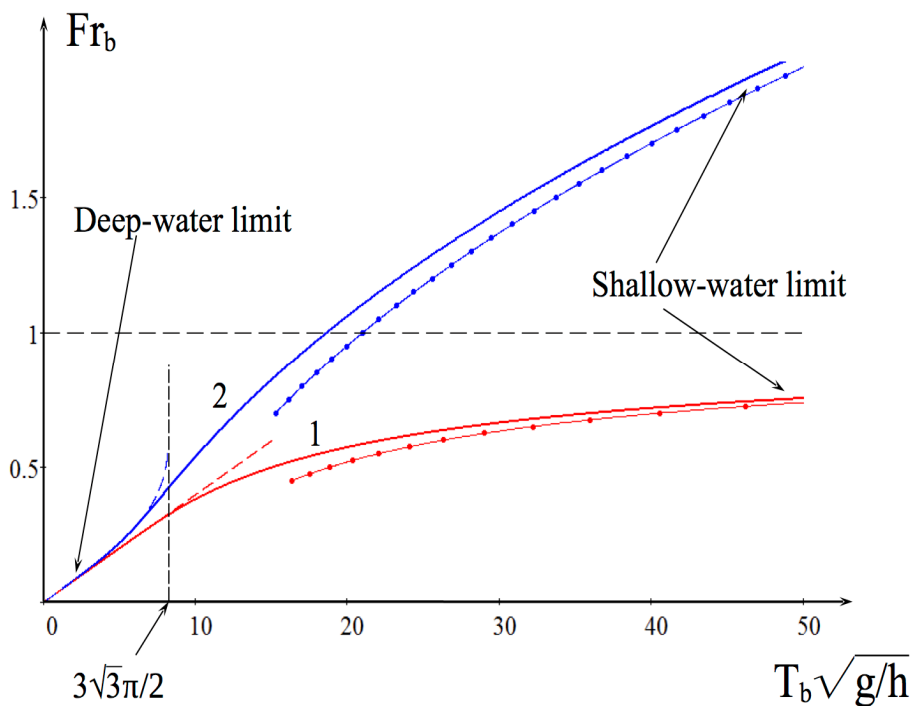

Figure 7. Froude number for the blocking (indexed by b) phenomenon as a function of dimensionless period (the surface tension effect is neglected). Line 1 – uniform flow without vorticity; line 2 – flow with constant vorticity and $\alpha = 1$. Horizontal dashed line is the shallow water asymptote U_h when $T_b \to \infty$.

The blocking Froude number (written in terms of the surface velocity U_0) in the general case of a shear flow with a constant vorticity is given asymptotically, when it approaches the limiting value

$$U_{\lim} = -\sqrt{\frac{gh}{1-\alpha}}, \tag{4}$$

by the following formula:

$$U_0^* \approx -\sqrt{\frac{gh}{1-\alpha}}\left\{1 - \left[\frac{2\sqrt{2}}{3\pi}\sqrt{\frac{g}{h}}T\frac{(1-\alpha)^2}{2-\alpha}\right]^{-2/3}\right\}, \tag{5}$$

where $\alpha = \Omega h / U_0$ – the dimensionless vorticity parameter. In the case of no vorticity ($\alpha = 0$) this formula reduces to Eq. (2), and the limiting value of Froude number in this case is one. This dependence in terms of $Fr_b = U_0^*/(gh)^{1/2}$ is shown in Figure 7 by red line which asymptotically tends to the horizontal dashed line $Fr_b = 1$ when the wave period infinitely increases.

In another limiting case when the vorticity parameter $\alpha = 1$ (this corresponds to a shear flow with the linear vertical profile vanishing at the bottom), Eq. (5) is not applicable. In this case the accurate

consideration for the blocking velocity of surface flow U_0^* leads to following the asymptotic dependence valid at large periods:

$$U_0^* \approx -\sqrt{gh}\sqrt{\frac{\sqrt{2}}{3\pi}\sqrt{\frac{g}{h}}T}\,.$$

(6)

This dependence is shown in Figure 7 by the dotted blue line. Hence, the blocking Froude number in the presence of vorticity with $\alpha = 1$ is no longer a constant at large periods but is the function of wave period and water depth.

A particularly interesting feature of gravity-capillary waves is the possibility for them to penetrate directly into the region forbidden for pure gravity waves (Rousseaux et al., 2010; the threshold shown by vertical dashed line 5 in Figure 8) avoiding the double reflection scenario described by Badulin et al. (1983) and studied further by Trulsen & Mei (1993). The condition for direct penetration does not depend on the presence of nonzero vorticity (Maïssa et al., 2013).
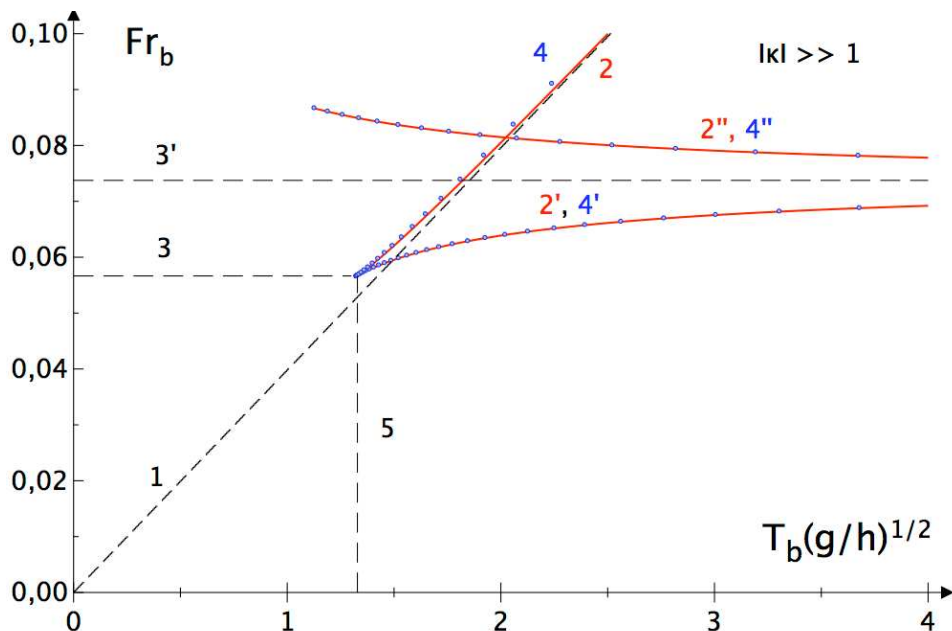

Figure 8. The same as in Figure 7 but with the effect of surface tension in deep water. Line 1 is the deep-water asymptote U_g; line 3' is the gravity-capillary asymptote U_γ.

6. Conclusions and perspectives

The problem of interaction between surface water waves and currents is rather old and classical. Nevertheless, new results were obtained recently by exploring the dispersion relation. We have presented the dispersive effects of water depth, surface tension, amplitude and vorticity. The existence of negative energy waves is a fact often overlooked in coastal processes. It would be of interest to compare our theoretical predictions with images of the free surface in the near shore region and in open oceans for which the presence of currents modifies the surface roughness and spectrum. Laboratory experiments in water channel would quantify the necessary discrepancies between our simplified approach and real world. Some other effects, which were ignored so far (e.g., viscosity, strong nonlinearity, influence of internal waves) should be also taken into consideration; this is the theme for the future work. A more detailed description of effects presented in this brief survey can be found in our paper (Maïssa et al., 2013), which will be available soon on ArXiv prior to publication in a journal.

References

Badulin S.I., Pokazeyev K.V. and Rozenberg A.D., 1983. A laboratory study of the transformation of regular gravity capillary waves in inhomogeneous flows. *Izv. Atmos. Ocean. Phys.*, 19, n. 10, 782–787.

Barenblatt G.I., 1996. Scaling, Self-Similarity, and Intermediate Asymptotics, *Cambridge University Press*, Cambridge.

Biesel F., 1950. Etude théorique de la houle en eau courante. *La Houille Blanche*, 5, 279–285.

Chawla A. and Kirby J.T., 2002. Monochromatic and random wave breaking at blocking points. Journal of Geophysical Research, 107, n. C7, 10.1029/2001JC001042.

Fabrikant A.L. and Stepanyants Y.A., 1998. Propagation of Waves in Shear Flows, *World Scientific*.

Jonsson I.G., 1990. Wave–current interactions, in B. Le Méhauté and D. M. Hanes, Ocean Engineering Science, The Sea, 9A, Wiley Interscience, pp. 65–120.

Karageorgis P., 2012. Dispersion relation for water waves with non-constant vorticity. *Eur. J. Mech. B Fluids*, 34, 7–12.

Kirby J.T. and Dalrymple R.A., 1986. An approximate model for nonlinear dispersion in monochromatic wave propagation model. *Coastal Engineering*, 9, 545–561.

Kovalev N.F., 1984. The linear theory of microwave devices with high-current beams of relativistic electrons moving straight. Relativistic High-Frequency Electronics, n. 4, Ist. Appl. Phys., Russ. Acad. Sci., Gorky, 3–48.

Maïssa P., Rousseaux G. and Stepanyants Yu., 2013. On the influence of shear-flow vorticity on the wave-current interaction. *Submitted*.

Nardin J.-C., Rousseaux G. and Coullet P., 2009. Wave-current interaction as a spatial dynamical system: analogies with rainbow and black hole Physics. *Phys. Rev. Lett.*, 102 (12): 124504-1/4.

Nezlin M.V., 1976. Negative-energy waves and the anomalous Doppler effect. *Sov. Phys. Uspekhi*, 19, 946–954.

Ostrovsky L.A., Rybak S.A. and Tsimring L.Sh., 1986. Negative energy waves in hydrodynamics. *Sov. Phys. Uspekhi*, 29, n. 11, 1040–1052.

Peregrine D.H., 1976. Interaction of water waves and currents, *Advances in Applied Mechanics*, 16, Academic Press, pp. 9–117.

Rousseaux G., Maïssa P., Mathis C., Coullet P., Philbin T. and Leonhardt U., 2010. Horizons effects with surface waves on moving water. *New Journal of Physics*, 12: 095018.

Rousseaux G., The Basics of Water Waves Theory for Analogue Gravity, 2013. *Editor Daniele Faccio, SIGRAV School on Analogue Gravity, Como, Italy*. Springer.

Stepanyants Yu.A. and Fabrikant A.L., 1989, Propagation of waves in hydrodynamic shear flows. *Sov. Phys. Uspekhi*, 32, n. 9, 783–805.

Skop R.A., 1987. Approximated dispersion relation for wave-current interactions. *J. Waterw., Port, Coastal, Ocean Eng.*, 113, 187–195.

Taylor G.I., 1955. The action of a surface current as a breakwater. *Proc. Roy. Soc. A*, 231, 466–478.

Thomas G.P. and Klopman G., 1997.Wave-current interactions in the nearshore region, in Gravity Waves in Water of

Finite Depth, J. N. Hunt, Editor, *Advances in Fluid Mechanics*, Vol. 10, CMP, Southampton.

Thompson P.D., 1949. The propagation of small surface disturbance through rotational flow, *Ann. N.Y. Acad. Sci.*, 5, 463–474.

Trulsen K. and Mei C.C., 1993. Double reflection of capillary-gravity waves by a non-uniform current: a boundary-layer theory. *J. Fluid Mech*., 251, 239–271.